A preliminary approach to the load and stress analysis of the arc-shaped corrugated steel structure

E. Narvydas*, N. Puodžiūnienė**

Kaunas University of Technology, Kęstučio 27, 44312 Kaunas, Lithuania, E-mail: Evaldas.Narvydas@ktu.lt
**Kaunas University of Technology, Kęstučio 27, 44312 Kaunas, Lithuania, E-mail: Nomeda.Puodziuniene@ktu.lt*

1. Introduction

According to data of American Iron and Steel Institute [1], compared with other materials such as timber and concrete, the following advanced qualities are characteristic for the cold-formed steel structural members: lightweight; high strength and stiffness; ease of prefabrication and mass production; fast and easy erection and installation; economy in transportation and handling; recyclable material etc. Standardized single-story metal buildings have been widely used in industrial, commercial, and agricultural applications. However, the self-supporting arc-shaped corrugated steel panels became widely used for roofs or entire buildings only in recent years, and the load-bearing characteristics of these structures are not fully defined yet [2, 3]. The main reasons of unconventionally complicated load-bearing behaviour of such panels are: a complicated geometry that includes the transverse corrugation, an effect of cold deformation on the materials properties of the panel and, possibly, the complex loads during the service life of the structure. Various simplifications of a mathematical formulation and an experimental setup of the arc-shaped corrugated steel panel under the load gave different and, sometimes, contradictory results.

L. Xu, Y.L. Gong and P. Guo have published results of compressive tests of cold-formed steel curved panels [4]. After the comparison of the ultimate load results of panels with transverse corrugation (crimples) to the panels without the transverse corrugation, it was concluded that the transverse corrugation reduces ultimate load capacities of the panels (ultimate load of corrugated panels comprises 72-105% of the straight panels without crimples). The similar conclusion was drawn by P. Casariego at al [3] based on a simplified finite element models of the panel with transverse corrugations and without it. The analysed panel under compression and under the bending showed a significant influence of the transverse corrugation on the

ultimate load. Depending on case, the ultimate load of the smooth panel differed from the corrugated one from 1.6 to nearly 2 times. L.L. Wu at al [5] analysing corrugated steel panels concluded that the corrugation increases a critical load of local buckling; however, the post buckling behaviour of such panels demonstrates a sudden breakdown. The discrepancy of the results of corrugated steel panel load-bearing capacities allows to conclude, that the results are very sensitive to the conditions of real or simulated experiment – geometry simplification, loading and fixture of the panel, and a definition of the material properties in case of numerical simulation.

The presented work targets the task to find how the panels behave under the loads applied on the full-scale model of the structure, instead of investigating the simplified examples of a separate panel. The loads of the full-scale structure primarily were based on the Lithuanian national code STR 2.05.04:2003 (Technical Regulation of Construction: Actions and loads) [6] and also related to the Eurocode EN 1991 (Eurocode 1): Actions on structures [7] and Eurocode EN 1990 (Eurocode 0): Basis of Structural Design [8].

The full-scale model served for the initial structural analysis of the assembly and, therefore, was simplified to represent only a global stress distribution. The model parameterization and optimization methodology in the conceptual design stage have been recently presented by S. Arnout at al [9]. After the preliminary analysis and optimization of the full-scale model, the most loaded panel can be separated from the assembly with the boundary conditions transferred from the full-scale model. Then, the design model (parameterized geometry) and the analysis
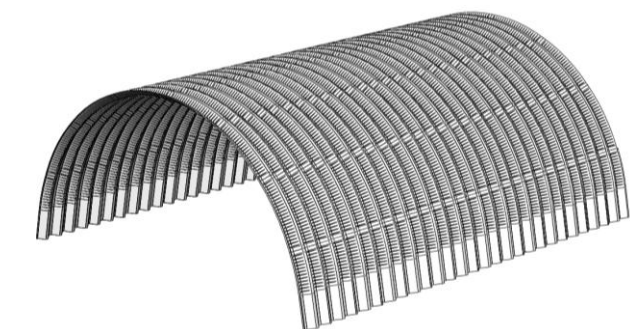

a

b

Fig. 2 General view of the corrugated steel panel (a) and dimensions of the cross-section (b)

Fig. 1 Assembly of the ach-shaped corrugated steel panels constructing a self-supporting building structure

model (finite element model) of the separated panel can be significantly refined for the further analysis.

2. Design of the arc-shaped corrugated steel structure

The analysed thin-walled structure had an overall shape of a semi-cylinder (Fig. 1). The structure was assembled from the arcs and each arc was constructed of the arc-shaped corrugated steel panels produced by cold forming from the 2500×1500 mm sheets (Fig. 2). The curved panel had the straight zones at the ends of 200 mm length that were overlapping in the arc assembly. The panel thickness was 0.8 mm. The geometry of cross-section of the panel is shown in Fig. 2, b. The cross section parameters were as follows: $L1 = 1180$ mm, $L2 = 50$ mm, $L3 = 187$ mm, $L4 = 92$ mm, $L5 = 100$ mm, $\alpha = 45°$. The first ant the last panels, constructing the arc, had the prolonged straight ends of 1000 mm length. The panels had the transverse corrugation in order to form the arched shape by cold forming.

3. Simplified model for parametric design and analysis

The transverse corrugations complicate the geometry of the panels and, subsequently, the whole structure. That makes almost impossible to build a full-scale finite element model according to the original shape; at least the model that could be used for the analysis in a rational time limits employing the contemporary numerical analysis tools. Certain degree of simplification is needed even for a model of a section of the one panel [5].

In the presented work, for the preliminary design stage, the transverse corrugation was neglected and the cross-section properties were set as constants. The main parameters were the radius of the arch R and the length of the structure b (Fig. 3). The length of the straight part of

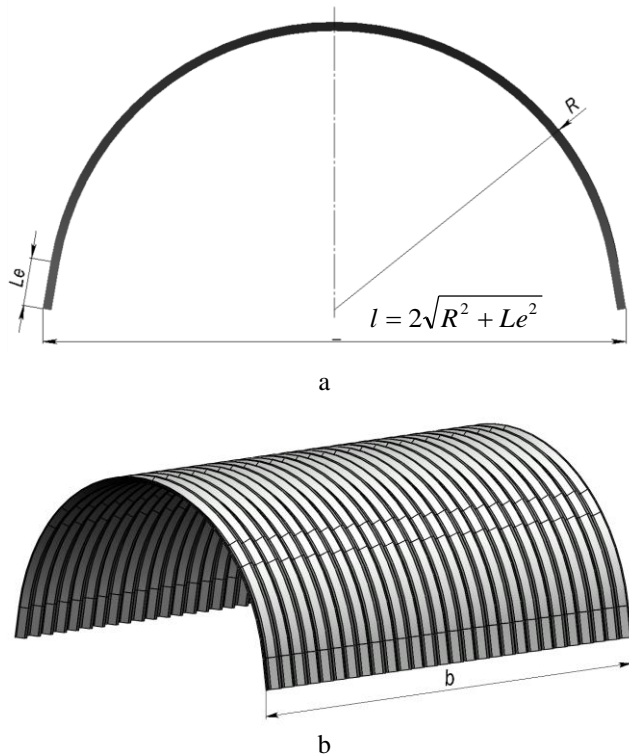

$$l = 2\sqrt{R^2 + Le^2}$$

a

b

Fig. 3 Simplified parametric design model of the structure: front (a) and isometric (b) views
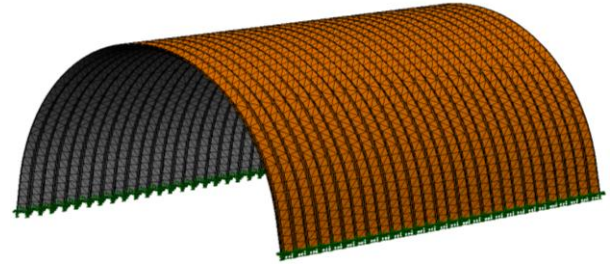

Fig. 4 View of the finite element model of the structure

the arcs was set to be constant ($Le = 1000$ mm). The R changes in a discreet way, because the arcs are assembled from the separate overlapping panels. It was assumed to consider the structures, where arcs are assembled from 5 to 12 panels in this analysis, therefore, the range of R was from 3724 to 8849 mm. The b was assumed to be not less than the width of the arc ($b \geq l$; Fig. 3).

The analysis model (Fig. 4) was created using *SolidWorks Simulation* software. Triangular shell type finite elements having six nodes were employed. Displacement interpolation inside the element follows the second order parabolic element shape function. The element neglects the transverse share effect i.e. uses a "thin" formulation based on the discrete-Kirchhoff approach [10]. All nodal degrees of freedom were constrained at ends of the arcs. The uniform thickness (0.8 mm) of the shell was assumed for the entire model.

The material of the structure was a hot-dip galvanized steel DX51D, EN 10327-2004. The minimal mechanical characteristics presented by the certificate of the steel supplier were: yield stress point 310 MPa, tensile strength 375 MPa, elongation after fracture 29%. The physical properties of this steel were: Yong's modulus 205000 MPa and Poison's ratio 0.29.

4. Loads

The loads were applied on the structure considering Lithuanian national code [6], Eurocode 1 and Eurocode 0 [7, 8]. According to these codes, there are service, gravity (self-weight), snow and wind loads acting on the structure. The priority is given to the national code in this analysis.

4.1. Self-weight

The self-weight of the structure was accounted including gravity load in the finite element model – applying density of the material $\rho = 7870$ kg/m^3, gravitational acceleration 9.81 m/s^2 and geometry of the modeled structure.

4.2. Snow load

According to Eurocode 1, part 1-3 and national code STR 2.05.04:2003, the snow load on the roof is calculated by Eq. (1):

$$s = \mu_i \, C_e \, C_t \, s_k, \tag{1}$$

here μ_i is a roof shape factor, C_e and C_t denote the exposure and thermal factors, usually considered as unity, and s_k is a characteristic snow load on the ground. The s_k value
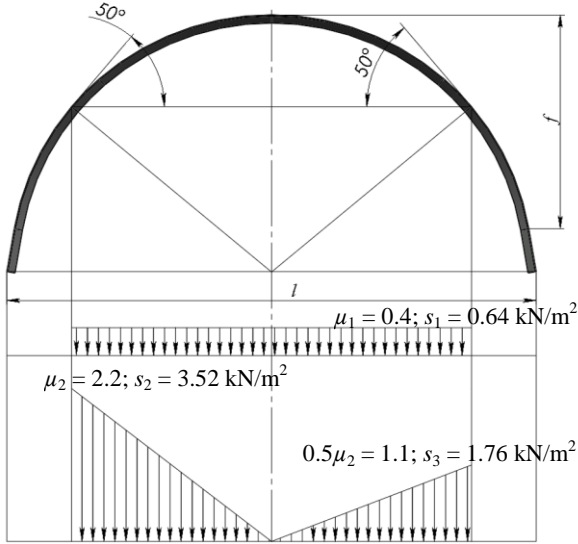
Fig. 5 Scheme of the snow loads

depends on the country region and was selected equal to 1.6 kN/m² in this analysis (Annex 1 of the national code STR 2.05.04:2003). The factors C_e and C_t were assumed equal to 1. The factor μ_i for the arched shape roofs depend on the parameters f and l (Fig. 5). For the planned structure, f is in a range from 3 to 8 m; the relation $1/8f < 0.4$ and $f/l \geq 1/5$. Therefore, the shape factor for the uniformly distributed load $\mu_1 = 0.4$ and the shape factor for the drifted snow load $\mu_2 = 2.2$. The loading schemes are presented in Fig. 5. The values of the snow load at critical points of the loading schemes, calculated employing Eq. (1), are: $s_1 = 0.64$ kN/m², $s_2 = 3.52$ kN/m² and $s_3 = 1.76$ kN/m² (Fig. 5).

4.3. Wind actions

The wind actions on structures are determined by Eurocode 1, part 1-4 and the national code STR 2.05.04:2003 with Annexes 3 and 4. The determination of the wind actions starts from the evaluation of the basic wind velocity. According to the standards, the basic wind velocity:

$$v_{ref} = c_{DIR} \cdot c_{TEM} \cdot c_{ALT} \cdot v_{ref,0} , \qquad (2)$$

here $v_{ref,0}$ is a fundamental value of the basic wind velocity; c_{DIR} is the directional factor, c_{TEM} is the season factor and c_{ALT} is the altitude factor. All these factors were accepted as equal to 1. The fundamental values of the basic wind velocity are given in the Annex 3 of the national code and the value of 24 m/s was accepted for the calculations.

The expression of the basic velocity pressure is given by Eq. (3):

$$q_{ref} = \frac{\rho}{2} v_{ref}^2 , \qquad (3)$$

here ρ is an air density; $\rho = 1.25$ kg/m³ was used in this analysis. Then $q_{ref} = 0.36$ kN/m².

The mean velocity pressure acting on the external surfaces was evaluated using Eq. (4) [6]:

$$w_{me} = q_{ref}\, c(z)c_e , \qquad (4)$$

here $c(z)$ is a factor dependant on the terrain roughness and orography; c_e – aerodynamic coefficient for the external pressure. For the structure of interest, the A type of country region was assumed where the values of $c(z)$ are as follows: $c(z) = 0.75$, if $z \leq 5$ m and $c(z) = 1.0$, if $z = 10$ m, where z is the height.

Aerodynamic coefficients for the external pressure depend on the relations of the structure dimensions: h_1/l; f/l and b/l according to Annex 4 of the STR 2.05.04:2003 [6]. For the planed structure these relations are in the ranges: $h_1/l = 0 ... 0.2$, $f/l = 0.4 ... 0.5$, $b/l = 1 ... 2$. Changing the structural parameters, these relations changes and the aerodynamic coefficients should be recalculated.

4.4. Service load

Characteristic service load q_k was applied as shown in Fig. 6. Standard [6] also requires to check the roof of the structure against the concentrated load $Q_k = 1.5$ kN applied on 50×50 mm square.
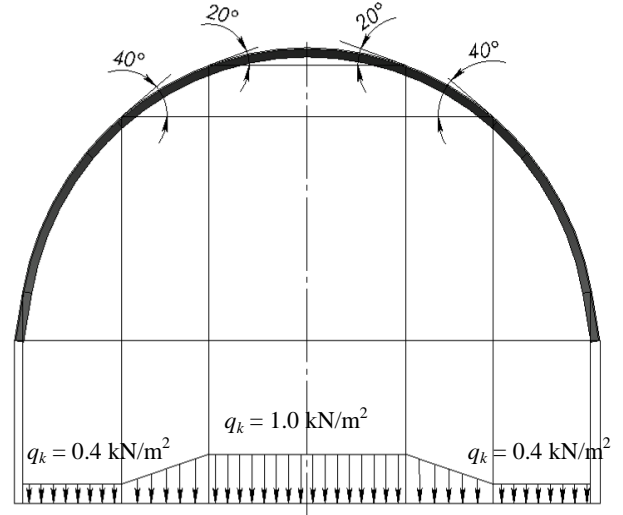

Fig. 6 Scheme of the distributed service load

4.5. Combination of actions

The structural design codes [6, 8, 10] require that the design value of the effect of actions (E_d) should not exceed the value of the corresponding resistance (R_d). The combination of effects of actions should be based on the following relation:

$$E_d = E\left\{\gamma_{G,j}G_{k,j};\gamma_p P;\gamma_{Q,1}Q_{k,1};\gamma_{Q,i}\psi_{0,i}Q_{k,i}\right\}, \quad j \geq 1, i > 1, \quad (5)$$

where the combination of actions in brackets { }, in Eq. (5), may be expressed as:

$$\sum_{j \geq 1}\gamma_{G,j}G_{k,j} \overset{''}{+} \gamma_p P \overset{''}{+} \gamma_{Q,1}Q_{k,1} \overset{''}{+} \sum_{i > 1}\gamma_{Q,i}\psi_{0,i}Q_{k,i}, \qquad (6)$$

here $G_{k,j}$ is the characteristic value of permanent action j; $Q_{k,1}$ is characteristic value of the leading variable action 1; $Q_{k,i}$ is characteristic value of the accompanying variable action i; P is representative value of a prestressing action; $\gamma_{G,j}$ is partial factor for permanent action j; $\gamma_{Q,1}$ is partial

factor for leading variable action 1; $\gamma_{Q,i}$ is partial factor for variable action i; γ_P is partial factor for prestressing actions; ψ_0 is factor for combination value of a variable action; "+" implies "to be combined with" and Σ implies "the combined effect of". For the presented case, there is no prestressing action applied on the structure and only the self-weight is treated as a permanent action. Having in mind that there are only three variable actions of different origin (service load, snow load and wind pressure) and that the service load should not be combined with snow load or wind actions, the expression (6) reduces and Eq. (5) becomes:

$$E_d = E\left\{\gamma_{G,}G_k{}^{"}+{}^{"}\gamma_{Q1}Q_{k1}{}^{"}+{}^{"}\gamma_{Q2}\psi_0 Q_{k2}\right\}, \qquad (7)$$

here $\gamma_G = 1.35$; $\gamma_{Q,1} = 1.3$ and $\gamma_{Q,2} = 1.3$ where the variable action is unfavorable; $\gamma_{Q,1} = 0$ and $\gamma_{Q,2} = 0$ where the variable action is favorable; $\psi_0 = 0.6$ for the wind actions and $\psi_0 = 0.7$ for the snow load (Annex 10 of STR2.05.04:2003 [6]).

5. Results of the parametric analysis

The considered loads: self-weight, service load, uniformly distributed snow load, drifted snow load and wind actions produce 10 different load combinations in total. It would be extremely time-consuming to use all possible load combinations in the parametric analysis. Review of the load combinations allow to conclude that the wind actions likely will produce a favorable effect and the uniformly distributed snow load will produce a less effect than the service load. Therefore, the two cases of the load combinations were selected for the preliminary parametric analysis: the case of the self-weight combined with the drifted snow load and the case of the self-weight combined with the distributed service load. Then, at the point where the critical (optimal) parameters are reached, the effects of all load cases were checked.

The maximal von Mises stress ($\sigma_{eq\,max}$) at the middle layer of the shell was considered as the effect of actions in the analysis. The resistance of structure $R_d = R_k/\gamma_M$. Here $\gamma_M = 1.1$ [11] is a partial factor for a material (sheet and profiled steel) property, and $R_k = 310$ MPa is a characteristic value of the resistance assumed to be equal to the yield stress of the material. Therefore, $R_d = 282$ MPa in this analysis.

After the preliminary parametric analysis, it was found, that the assumption of the linear relation between the maximal von Mises stress and the radius of the structure (structural parameter R, Fig. 3) can be used (Fig. 7). The dots present the finite element analysis results in the Fig. 7. The coefficient of determination for the linear fitting of the effect results for combined self-weight and the drifted snow load is 0.994 and, for the combined self-weight and the service load, it is 0.984 in a range of the structural parameter R from 4.5 to 8 meters. The critical value of the R, regarding the value of the resistance of structure, is 6013 mm. Therefore, the maximal arc of the structure would be assembled from 8 panels to make the actual maximal allowable $R_{all} = 5920$ mm in the acceptable design. The von Mises stress distribution under the
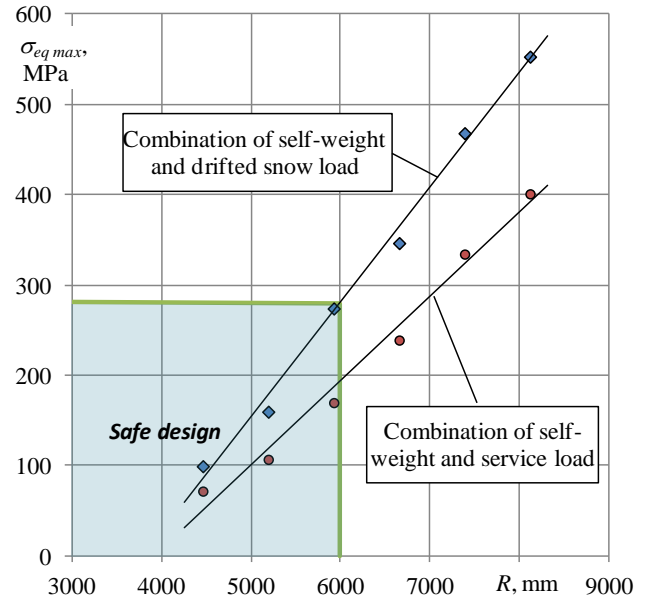

Fig. 7 Results of $\sigma_{eq\,max}$ versus R after the parametric analysis for selected combinations of actions
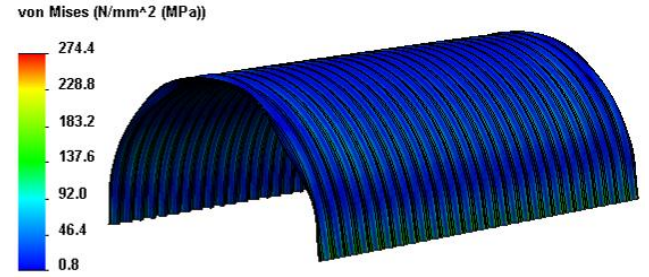

Fig. 8 Results of stress analysis under combined self-weight and drifted snow load ($R = 5920$ mm)

combined self-weight and drifted snow load is shown in Fig. 8. For this design case the all other possible load combinations were also tested, including the combinations with the wind actions, to be sure that the selected load combinations produces the highest stress levels in the structure.

The structure of R_{all} was divided in to five parts along the perimeter of the arcs to apply the wind pressure according to the national code [6]. The terrain roughness, orography factors and the aerodynamic coefficients for the external pressure defined by national code and the mean velocity pressure acting on the external surfaces calculated by Eq. (4) are presented in Table 1. The scheme of the external wind pressure on structure according to [6] is presented in Fig. 9. Results of the maximum stresses after the shell stress analysis for the all load combinations are presented in Table 2.

Table 1

Data of the standardized wind actions

Part No	$c(z)$	c_e	w_{me}, N/m^2
1	0.75	0.8	216
2	0.75	0.573	154.7
3	0.796	-1.11	-318
4	0.75	-0.4	-108
5	0.75	-0.427	-115.3
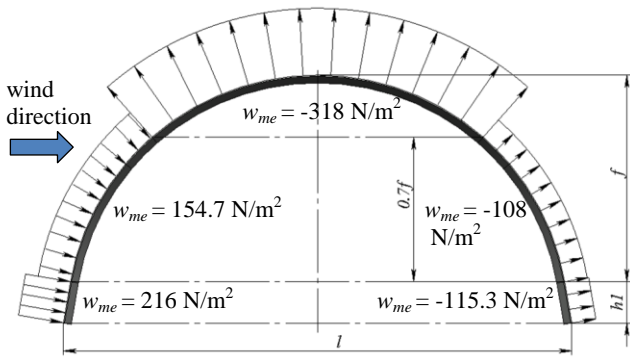
Fig. 9 Scheme of the standardized external wind pressure on the structure

Fig. 10 Stresses under load combination No. 6

Table 2

Maximum stresses for the load combinations

Load No	Load combinations	$\sigma_{eq\,max}$, MPa
1	Self-weight + uniform snow	124.7
2	Self-weight + drifted snow	**274**
3	Self-weight + service	170.1
4	Self-weight + wind	116.1
5	Self-weight + uniform snow + + wind	121.0
6	Self-weight + drifted snow + + wind side 1 (left)	**267**
7	Self-weight + drifted snow + + wind side 2 (right)	231
8	Self-weight + wind + + uniform snow	80.5
9	Self-weight + wind side 1 + + drifted snow	182.7
10	Self-weight + wind side 2 + + drifted snow	97.5

Fig. 11 Air pressure around the structure – side view

The other structural parameter, the length of the structure b (Fig. 3), was found to have a negligible influence in to the results when the $l \le b \le 2l$.

6. Comparison of standardized and simulated wind actions

Results of the stress analysis for the all load combinations demonstrate that the load combination No. 2 (Table 2) gives the highest stresses in the structure, but the load combination No. 6 is giving the maximal stresses (Fig. 10) only 2.5% lower. This load combination includes the wind actions defined by standard [6] (Fig. 9). Because the highest stresses of the two mentioned load combinations are so close to each other, the applied wind pressure was checked simulating the wind actions with the computational fluid dynamics (CFD) software. The *SolidWorks Flow Simulation* computer program was used. The simulation results of the absolute air pressure surrounding the structure are presented in Figs. 11-13. The atmospheric pressure was 101325 Pa and the air temperature 293.2 K. The wind direction is shown by arrows and the pressure distribution by the color map in the figures.

The aerodynamic coefficients calculated from the simulation results along the arc of the structure are pre-
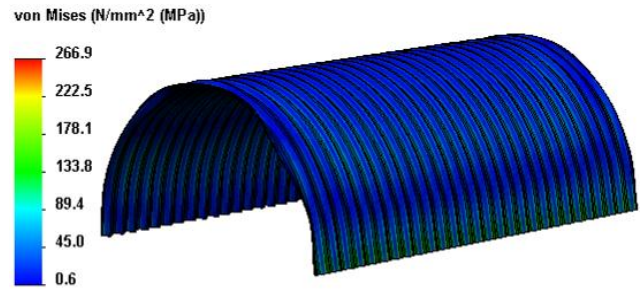

Fig. 12 Air pressure around structure – top view at the 2 m distance from the ground
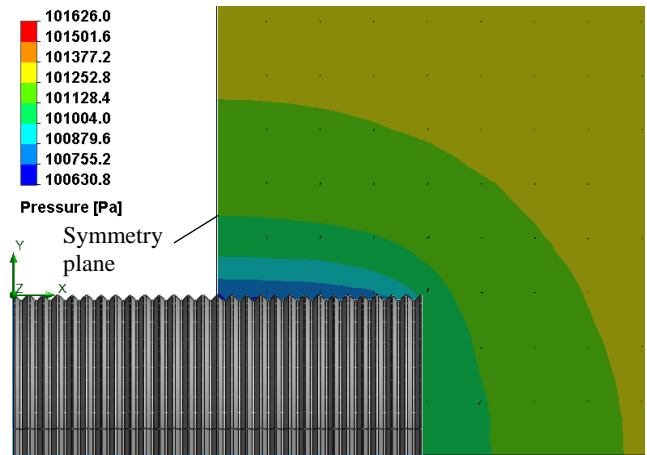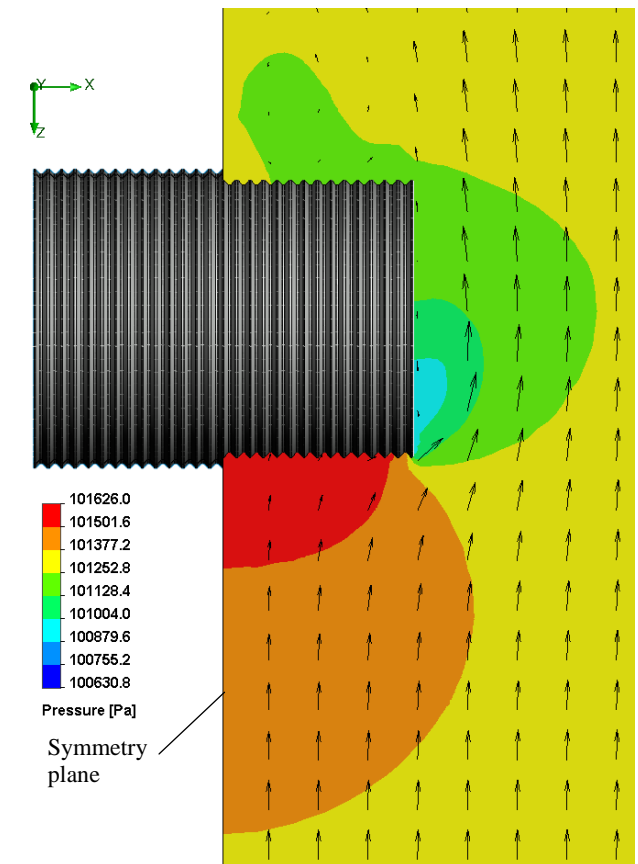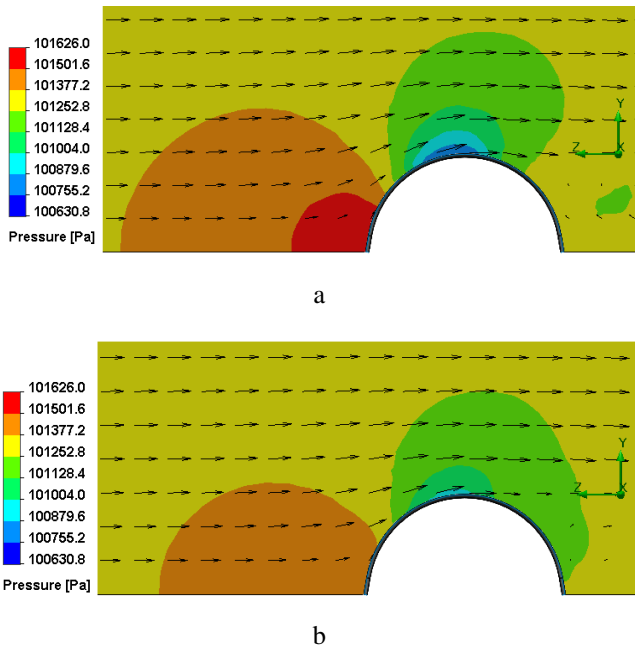
a

b

Fig. 13 Front view of the air pressure around the structure:
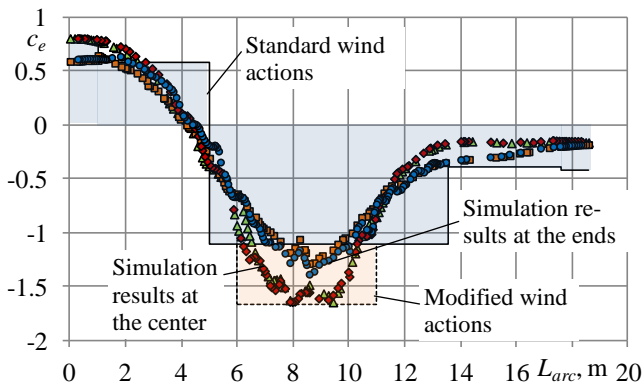a – at the center of the structure (at the symmetry plane), b – at the ends of the structure

Fig. 14 Aerodynamic coefficients for the external wind pressure along the arc of the structure defined by standard (solid line), calculated by CFD model (dots) and modified standard (dashed line)
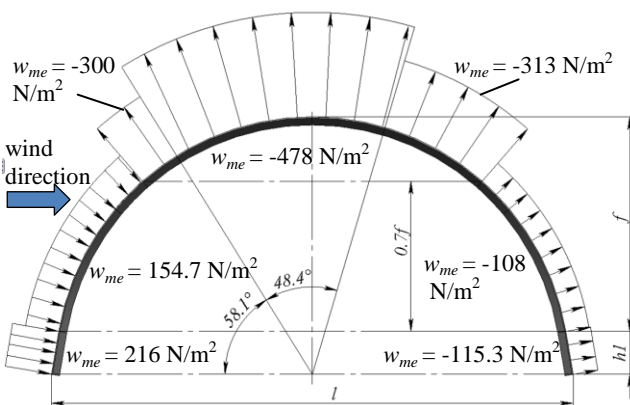

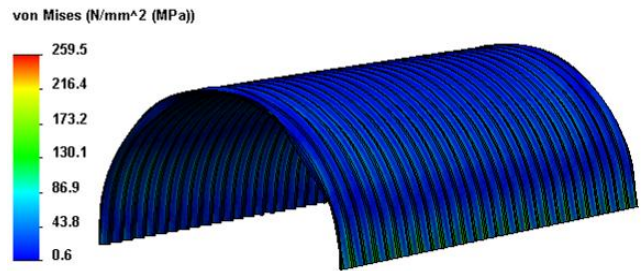Fig. 15 Scheme of the modified external wind pressure on the structure

Fig. 16 Stresses under load combination No. 6 with the modified wind actions

sented by dots in Fig. 14. These results show a drop of the absolute pressure at the ends the structure (Figs. 11-13). The solid lines (Fig. 14) represent the c_e calculated according to STR 2.05.04:2003 Annexes 4 [6] used in the preliminary analysis. Comparing the simulation results and the standard data it was defined that the c_e values obtained by simulation at the top of the structure (location along the arc from 6 to 11 m) are outside the range of the standard values. Because of this, the wind pressure on structure was refined dividing the structure along the arc in 7 parts. Dashed line (Fig. 14) shows the application rage of the c_e added to the earlier defined standard values (Table 1). The added value $c_e = -1.667$. The modified external wind pressure on the structure is presented in Fig. 15. One can compare it to the initially applied standard wind loads (Fig. 9). The stress plot under the load combination No. 6 with modified wind actions is presented in Fig. 16. The maximal stress calculated for this case $\sigma_{eq\,max} = 260$ MPa. It is 2.6% lower than earlier calculated value (267 MPa). This indicates that the modification of the wind actions had a little favourable effect for the structure.

7. Conclusions

A preliminary parametric load and stress analysis was performed for the simplified full-scale model of the self-supporting structure constructed from the corrugated arc-shaped panels. The most dangerous combination of loads was defined. The boundary conditions can be extracted from the results of the performed analysis for the further submodeling and geometry refinement of the structure.

The applied wind actions were defined following the standard requirements and alternatively defined by CFD simulation results. Some difference was found between standard wind actions and simulation results, however, the load combination with standard and simulated wind actions resulted only in 2.6% maximal stress difference in the structure. Besides, the simulated wind actions applied in the load combination gave a lower stress value.

The maximal value of the parameter R was defined for the simplified full-scale model (6013 mm). It means that maximum 8 panes of 2500 mm length with 200 mm overlap can be used to build the arc of this structure.

References

1. **Wei-Wen Yu.** 2000. Cold-formed steel structures, 3rd ed. New York: John Wiley and Sons. 768 p.
2. **Litong, S. Chen, L.** 2010. Computer nonlinear analysis

of ultimate bearing capacity of corrugated-arch metal roof. 2010 International Conference on Intelligent Computation Technology and Automation (ICICTA 2010). Proceedings of a meeting held 11-12 May 2010, Changsha, China. 1007-1010.
http://dx.doi.org/10.1109/ICICTA.2010.474.

3. **Casariego, P.; Casafont, M.; Muñoz, J.; Floreta, A.; Ferrer, M.; Marimon, F.** 2011. Failure mechanisms of curved trapezoidal steel sheeting. Proceedings of the EUROSTEEL 2011 6th European Conference on Steel and Composite Structures: research - design - construction, August 31 - September 2, 2011, Budapest, Hungary. 63-68.

4. **Xu, L.; Gong, YL.; Guo, P.** 2001. Compressive tests of cold-formed steel curved panels, Journal of Constructional Steel Research 57: 1249-1265.
http://dx.doi.org/10.1016/S0143-974X(01)00048-7.

5. **Wu, L.L.; Gao, X.N.; Shi, Y.J.; Wang Y.Q.** 2006. Theoretical and Experimental Study on Interactive Local Buckling of Arch-shaped Corrugated Steel Roof, International Journal of Steel Structures 6: 45-54.

6. STR 2.05.04:2003. 2003. Technical Regulation of Construction. Actions and loads. Vilnius: Ministry of Environment (in Lithuanian).

7. EN 1991. Actions on structures (Eurocode 1). European Committee for Standardization, CEN.

8. EN 1990. Basis of Structural Design (Eurocode 0). European Committee for Standardization, CEN.

9. **Arnout, S.; Lombaert, G.; Degrande, G.; De Roeck, G.** 2012. The optimal design of a barrel vault in the conceptual design stage, Computers and Structures 92-93: 308-316.
http://dx.doi.org/10.1016/j.compstruc.2011.10.013.

10. **Bathe, K.J.; Dvorkin, E.; Ho, L.W.** 1983. Our discrete-Kirchhoff and isoparametric shell elements for nonlinear analysis – an assessment, Computers and Structures 16: 89-98.
http://dx.doi.org/10.1016/0045-7949(83)90150-5.

11. STR 2.05.08:2005. 2005. Technical Regulation of Construction. Design of steel structures. Basic rules. Vilnius: Ministry of Environment (in Lithuanian).

E. Narvydas, N. Puodžiūnienė

ARKINĖS GOFRUOTO PLIENO KONSTRUKCIJOS PRELIMINARI APKROVŲ IR ĮTEMPIŲ ANALIZĖ

R e z i u m ė

Iš lakštinio plieno šaltuoju formavimu pagamintos plonasienės gofruotos arkinės konstrukcijos turi daug teigiamų savybių. Joms nereikia papildomų apkrovas atlaikančių elementų, tačiau nustatyti jų stiprumą ir stabilumą yra sunku. Skaičiavimus ypač apsunkina arkos formavimo metu sudaromi nedideli skersiniai įlenkimai – skersinis gofravimas, kuris gali turėti nemaža įtakos konstrukcijos stiprumui ir stabilumui.

Straipsnyje pateikta preliminarios analizės, atliktos, naudojant supaprastintą konstrukcijos modelį, dalis. Pridėjus techniniuose reglamentuose numatytus apkrovų derinius atliktas preliminarus įtempių skaičiavimas, nustatyti pavojingiausi apkrovų deriniai, apskaičiuotas maksimalus leistinas konstrukcijos lanko spindulys. Dėl pavojingų įtempių, susidarius savojo svorio, netolygiai supustyto sniego ir vėjo apkrovų deriniui, vėjo apkrova buvo patikslinta naudojant skysčių ir dujų mechanikos modeliavimo programą. Patikslinus vėjo apkrovą, šiek tiek sumažėjo maksimalūs įtempiai dėl palankaus vėjo apkrovos pobūdžio poveikių derinyje.

E. Narvydas, N. Puodžiūnienė

A PRELIMINARY APPROACH TO THE LOAD AND STRESS ANALYSIS OF THE ARC-SHAPED CORRUGATED STEEL STRUCTURE

S u m m a r y

Thin-walled arc-shaped corrugated steel structures, produced by cold forming, have many attractive features. These structures are self-supporting, however, the stress and buckling analysis is complicated due to transverse corrugations formed during the arc bending operation.

The paper presents the preliminary stage of the analysis of the simplified full-scale model of the arc-shaped structure. Applying load combinations defined by the standards, the preliminary stress analysis was performed, the most dangerous load combinations were defined, and the maximal allowable arc radius of the structures vault was calculated. Because of the high stress level under the load combination that includes the self-weight, drifted snow load and wind pressure, the wind load was calculated employing CFD simulation software and obtained results compared to values initially defined by standard requirements. The wind action was corrected regarding the simulation results; however it resulted in the insignificant stress reduction in the structure due to favorable effect of the wind load in the combination of actions.